© Universiti Tun Hussein Onn Malaysia Publisher's Office

IJIE

Journal homepage: http://penerbit.uthm.edu.my/ojs/index.php/ijie
ISSN : 2229-838X e-ISSN : 2600-7916

The International Journal of Integrated Engineering

LSTM-Based Electroencephalogram Classification on Autism Spectrum Disorder

N. A. Ali[1], A. R Syafeeza[2*], A. S. Jaafar[2], S. Shamsuddin[3], Norazlin Kamal Nor[4]

[1]Fakulti Teknologi Kejuruteraan Elektrik dan Elektronik (FTKEE)
Universiti Teknikal Malaysia Melaka (UTeM), 75450 Ayer Keroh, Melaka, MALAYSIA

[2]Fakulti Kejuruteraan Elektronik dan Kejuruteraan Komputer (FKEKK)
Universiti Teknikal Malaysia Melaka (UTeM), 76100 Durian Tunggal, Melaka, MALAYSIA

[3]Fakulti Kejuruteraan Pembuatan (FKP)
Universiti Teknikal Malaysia Melaka (UTeM), 76100 Durian Tunggal, Melaka, MALAYSIA

[4]Department of Paediatrics, Faculty of Medicine,
Hospital Censelor Tuanku Mukhriz (HUKM), 56000 Cheras, Kuala Lumpur, MALAYSIA

*Corresponding Author

DOI: https://doi.org/10.30880/ijie.2021.13.06.028
Received 18 February 2021; Accepted 25 May 2021; Available online 31 August 2021

Abstract: Autism Spectrum Disorder (ASD) is categorized as a neurodevelopmental disability. Having an automated technology system to classify the ASD trait would have a huge influence on paediatricians, which can aid them in diagnosing ASD in children using a quantifiable method. A novel autism diagnosis method based on a bidirectional long-short-term-memory (LSTM) network's deep learning algorithm is proposed. This multi-layered architecture merges two LSTM blocks with the other direction of propagation to classify the output state on the brain signal data from an electroencephalogram (EEG) on individuals; normal and autism obtained from the Simon Foundation Autism Research Initiative (SFARI) database. The accuracy of 99.6% obtained for 90:10 train:test data distribution, while the accuracy of 97.3% was achieved for 70:30 distribution. The result shows that the proposed approach had better autism classification with upgraded efficiency compared to single LSTM network method and potentially giving a significant contribution in neuroscience research.

Keywords: Deep learning algorithm, brain signal, electroencephalogram, autism spectrum disorder

1. Introduction

Autism Spectrum Disorder (ASD) is a neurodevelopmental disability that affects a child with symptoms of behavior. Childhood-onset of ASD occurs in the first year of life. It begins early in childhood when there is little social interaction and poor language development. The number of ASD children is rising annually in Malaysia and worldwide. The Ministry of Health (MOH) announced that in Malaysia, One in every 600 children was diagnosed with an autism spectrum disorder in 2004 [1]. In the more advanced nations like the United States, the Centers for Disease Control and Prevention (CDC) estimates that 1 in every 68 children is diagnosed with ASD, and the prevalence in the United Kingdom (UK) recorded that 1 in every 100 children has ASD [2]. Clinical specialist and paediatrics usually perform a continuous character, and behavioural evaluation in ASD diagnosis process and these may take a longer time in confirming the diagnoses.

*Corresponding author: syafeeza@utem.edu.my

A recorded paediatrics study indicated that a two-years old autistic child is still unable to produce two meaningful words which need not to be imitated or even repeated [3]. The exact reasons for the existence of this disorder remain unanswered, despite so much research being conducted. Autism Spectrum Disorder diagnoses are very complicated because it is not an inherited. ASD is defined as unusual, abnormal and episodic behavior, which typically begins at a young age and continues into childhood [4]. Detection is thus extremely unlikely prior to the age of three. Sometimes, ASD could also be mistaken with other neurodevelopmental symptoms. Maybe due to the little obvious variations in the primary neural conditions itself, this atypical behavior is so difficult to identify.

The Electroencephalogram (EEG) is a brain activity measurement device representing the brain electromagnetic signals state. According to Liu [5], the frequency of autistic children's brain waves shows a decrease in both their functional complexity and synchrony with the brain development. Studies carried out in [6–8] observed that there were noticeable differences found between the right and the central side of brain areas. Previous studies have shown that there is a relationship between autistic and non-autistic brain EEG signals [9–13].

Previous research in [8] revealed that the EEG recording could provide information that can benefit scientist in fields such as neuroscience compared to functional Magnetic Resonance Imaging (fMRI) due to the higher temporal resolution, lower complexity, lower cost and being an acceptable technique. In addition, the EEG is much superior inaccessibility than Magnetoencephalogram (MEG) since the dataset is more widely available [14-16]. As stated in [16], EEG is a useful method used to investigate the brain function in healthy individuals and those who are mentally impaired. EEG can rigorously analyze rest and active state of brain activity [17]. Additionally, the EEG may reveal which areas of the brain are actively involved in particular activities and is effective through it [18-19]. Another way to illustrate this is, for example, if you are in a happy mood, it not only causes part of your brain to 'happy' hormones to be released but that it also causes your face to smile or laugh. This is a simplistic illustration of how we are made to respond to brain activity. The brain signal of EEG is also a method used to identify changes in brain function. However, for the ASD individuals, it is as recorded otherwise by the EEG signal [20–23]. A study found that the apparently increased brain activation in the frontal and temporal lobes was the cause of the symptoms observed in children with autism [10]. Furthermore, a similar study indicated that it might be critical for both of these differences to be altered in order for behavioural symptoms of ASD to manifest. As stated in [24], ASD is triggered by a lack of functions in the frontal mirror neuron.

2. Methodology

2.1 Dataset

An institutional review board (IRB) review from our institution and the approval of the request for the EEG data on Simon Foundation Autism Research Initiative (SFARI) base. It was met with general approval after fulfilling the terms and conditions of the agreement and making the required statements and disclosures. SFARI obtained initial ethical approval for the Simons Variation in Individuals Project (SVIP). As part of the SVIP, approval was obtained for the data collection on individuals with 16p11.2 copy number variants (CNVs) and normal (non-autism) for their research data to be shared only with an approved researcher. The finding in this article represents the analyses of a previously collected dataset The Simons VIP Consortium, which was obtained via the SFARI upon data request process.

An Event-Related Potential (ERP) is the measured brain response that directly results from a specific sensory, cognitive, or motor event. The ERP of EEG recording taken in this study based on four tasks which are Visual Evoked Potential (VEP), Faces House (HF), Match Mismatch (MTH) and Congruent Incongruent (SEN) task. The dataset used in this work was collected on 128-channel HydroCel Geodesic nets at 500Hz sampling rate using NetAmps 300 amplifier. Eleven electrodes were removed marked as the missing channels and eye channels (eye blinks and eye movement) consists of channel 1,8,14,17,21,25,32,125-128. The remaining 117 channels being processed and performed in NetStation at 0.3-30Hz Bandpass filter. There are fourteen normal individuals (their ages 3-14years old) and thirty-nine cases (1-11years old). Dataset originally obtained from SFARI were 57 cases and 4 of them were excluded (2 individuals from each classes) in this work since contained a poor number of recording trials. Summary of the database is shown in Table 1 for each category, together with the number of good trials of four different tasks. The stimuli and procedure were as per described in earlier study in [33]. EEG recording and pre-processing steps performed prior to the study consisting of the refusal of obvious bad recording trial (three trials in total) based on manual visual inspection. These additional pre-processing steps were subsequently described in the section on the methodology presented in the following sub-section.

.Table 1 - Description of the EEG database on four different tasks

Genotype Case	Gender	Age	No. of Good Trial			
			VEP	HF	MTH	SEN
Normal (Non-autism)	Male-6 Female-8	Min:3 Max:14	910	267	188	267
Autism	Male-22 Female-17	Min:1 Max:11	2128	462	386	576

2.2 Proposed Method

Fig. 1 indicates the principal procedures for the proposed method. The following sections provide thorough explanations of each stage in this work.

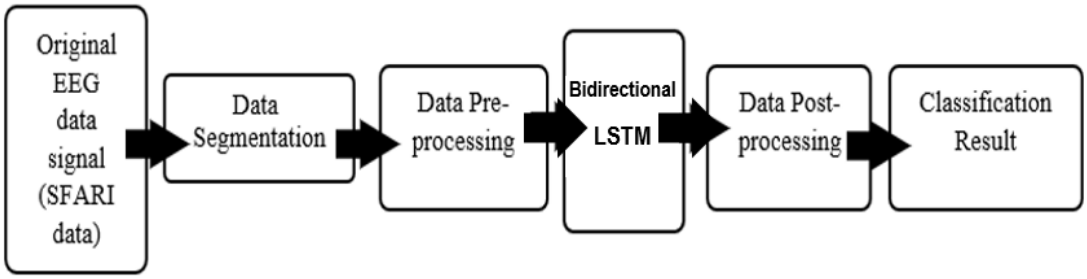

Fig. 1 - The proposed method structure diagram

2.2.1 Data Segmentation

In this work, the EEG signals collected from each channel are analyzed for both labels; normal (non-autism) and autism. Data obtained from the original SFARI will be converted in the form of MAT-files that contains EEG signals. A two variables were loaded into workspace contained Signals with obtained Labels: normal (N) and autism (A).

Signals are a cell array containing the EEG channels, which totalled 117 channels (after removing all the poor channel) for each case. Label is an array of groups containing the necessary ground truth signal labels. For these EEG signals of a particular channel, the EEG data signals were segmented from originally 200k signal samples to 5k signal samples each and labelled in consecutive order for both as normal and autism. These segmented signals essentially have their own labels based on the original type of signal previously present.

2.2.2 Data Pre-processing

For any deep-learning-based approach, data pre-processing is crucial as the real-world involves incomplete, noisy, and inconsistent data. Poor quality of data can lead to poor classification.

The training and validation sets were chosen according to the 90:10 and 70:30 data distribution ratios for each patient. The dataset is identical in length that is being augmented to train the proposed deep learning algorithm on a bidirectional-LSTM network, while the remaining normal and autism EEG data has been considered as the testing data to validate its output. There were 53 subjects (normal and autism) in total of the EEG data consisting of 117 channels for each case. The EEG data distribution is used both to train and test the deep learning model output performance. Listed in Table 2, the distribution of training and test data along with the segmented data

Table 2 - Distribution of the segmented data samples

Genotype Case	Segmented data	Distribution	90:10	70:30
Normal (Non-autism)	524	Training	472	367
		Test	52	157
Autism	1565	Training	1408	1096
		Test	157	469

2.2.3 Bidirectional-LSTM Network

The term LSTM refers to a Long-Short-Term-Memory. It is a deep learning system under artificial intelligent (AI). It can be used to address issues associated with the Recurrent Neural network (RNN) model, in terms of replacing the updates of hidden layers with its mechanism of gates and memory cells. LSTM networks can acquire dependencies of a long-term sequences data between the interval of time [32]. As Fig. 2 shows, inside a single LSTM block consists of three gates called input, forget and output gates. The input gate decides to specify if present state condition on the block is modified using a sequence of input. The forget gate is used to hold or delete the prior condition on the LSTM block while the output gate tracks the information output and decides whether the current hidden state is moved to the next restatement.

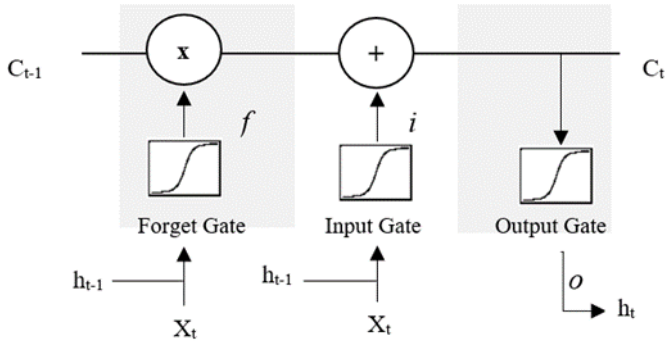

Fig. 2 - LSTM internal block structure [32]

The activation function used by these three gates is sigmoid, which produces values between 'zero' and 'one', whereby '0' implies the gate is closed and it passes no information through while '1' does the contrary. During the training phase, both bias (*b*) and weight matrix (*w*) are updated. The equation for the LSTM gates expressed as:

$$i_t = \sigma\left(w_i\left[h_{t-1}, x_t\right]\right) + b_i \quad (1)$$

$$f_t = \sigma\left(w_f\left[h_{t-1}, x_t\right]\right) + b_f \quad (2)$$

$$o_t = \sigma\left(w_o\left[h_{t-1}, x_t\right]\right) + b_o \quad (3)$$

where i_t, f_t and o_t denotes the gate's input, forget and the output. The LSTM network typically collects data from the previous input, without using data from the future possible input. The bidirectional-LSTM network which made up of two separate blocks, not only relay information front-to-back, but also back-to-front data and the output value is computed together. Thus, in working with the EEG data that have the pre-and-post dependencies, this deep model can achieve excellent performance.

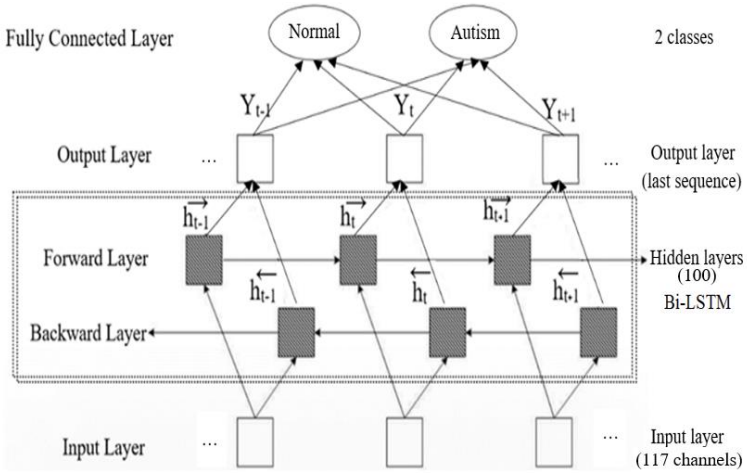

Fig. 3 - Proposed bidirectional-LSTM network structure

Fig. 3 demonstrates a deep network of bidirectional-LSTM network is designed. The ($h_t\rightarrow$) in the forward layer portrays the first LSTM block with front-to-back passed information, while the ($h_t\leftarrow$) represents the backward layer of final LSTM block with back-to-front information transferred. The input layer consists of all 117 channels of EEG signal while output layer Y_t specify the last sequence of output. The sequence in both forward and reverse directions bidirectional-LSTM is used in this work (as illustrated in the rectangular box with a dotted line). The brain signal from the dataset indicates the one-dimensional (1D) array for each channel, so the input size specified to be sequences of size one. An LSTM network with a hidden layer with an output size of 100 and the output of the last element of the sequence was specified.

The architecture of this proposed network allows the information to be saved for a long time in memory units. It can also process information in both directions, allowing for the full use of both preceding and following information. The input series will then be mapped into 100 features by this proposed network model and the output will be generated for the fully connected layer. Finally, two classes labelled as normal and autism were specified by including a fully connected layer of size 2, connected by a classification and softmax layers as its activation function. A training option

classifier has been developed. The maximum epoch been set to 10 to allow the network to make 10 training passes since the dataset larger size in amount., A mini-batch size is set at 150 to ensure a hundred and fifty training signals at a time. Since the mini-batches have long sequences, the 'Execution of environment' is set to 'single GPU' to train the dataset on a GPU. It much faster compared to running by a CPU. The 0.01 of learning rate helped the training process speed up. When many pieces of data are being analysed at once, a 1,000-point cycle period is used to divide the signal into smaller bits so the computer does not use up all of its memory capacity by looking at too many data. This work also used the Adaptive Moment Estimation (ADAM) optimizer since it fits best with RNNs as it requires less memory than the default Stochastic Gradient with Momentum (SGDM) solver as the optimizer.

2.2.4 Data Post-processing

Since EEG signals have previously been tested by maximum epoch, the deep bi-LSTM network will generate a sequence of successive decision variables. The proposed network connected to the previously mentioned training option and layer architecture were trained using the function of trainingNetwork. As the training set is big, the training phase on signal data was processed for several hours. The same processes repeated for a single LSTM network and the comparison in these two recorded in the accuracy graph tabulated in Result section.

2.3 Performance Measure

The efficiency of classification is measured in terms of few performance measure such as overall accuracy, sensitivity and precision. Confusion matrices are used in classification problems to visualize the output of a classifier on a set of data recognized for the true values. The Predicted Class is the signal's ground-truth label and the Output Class is the label the network applied to the signal. Two axes labels reflect the class labels of cases in this study: Normal for control case and Autism. The classification performance is visualized in confusion matrix. Table 3 demonstrates the possible answers for a prediction and actual class for both cases.

Table 3 - Confusion matrix on Autism prediction

Actual Class	Predicted Class	
	Autism	**Normal**
Autism (A)	True Positive (TP)	False Negative (FN)
Control (N)	False Positive (FP)	True Negative (TN)

The proposed network model's accuracy on the signals was demonstrated through the classification of training data. On a given test dataset, the accuracy of a classifier is the percentage that the classifier classifies the test dataset correctly. The following statistical indicators used in this study:

$$Accuracy = \frac{TP + TN}{TP + TN + FP + FN}$$

$$Sensitivity = \frac{TP}{TP + FN}$$

$$\Pr ecision = \frac{TP}{TP + FP}$$

3. Result and Discussion

3.1 Data Signal

Based on the obtained database which were collected on 128-channel HydroCel Geodesic nets sampled at 500Hz sampling frequency. Eleven channels have been extracted with originally obtained 128 recorded electrodes; marked as missing and eye artifact removal channels as mentioned previously. The remaining 117 channels are being processed, and these segments from these signals are represented in Fig. 4 for a single person in both the normal and autism classes. As for five thousand of signal sampled data, the autism brain signals are scattered irregularly, while the brain signals of normal person occur regularly.

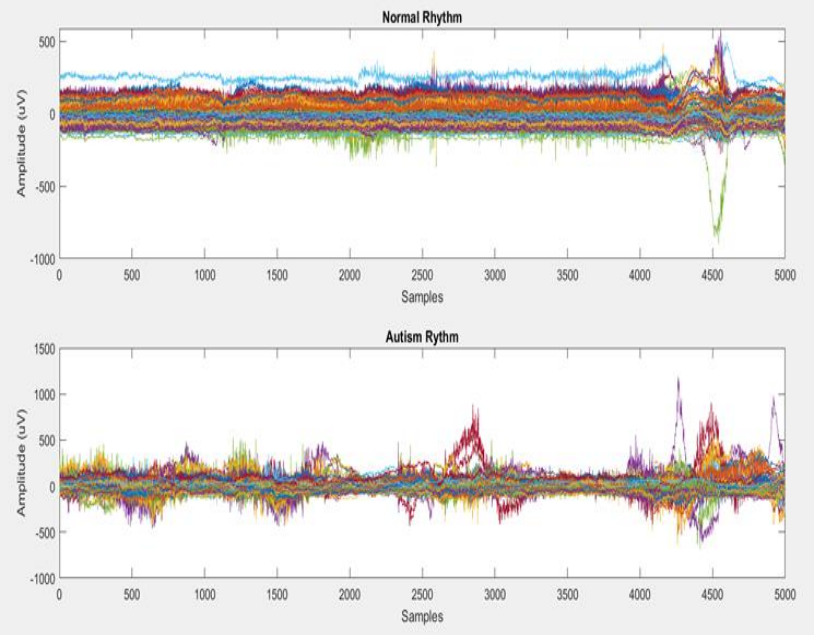

Fig. 4 - The plotted figure represents rhythm signals on control (normal) and autism

3.2 Training Results

Fig. 5(a) and Fig. 5(b) show the accuracy and loss graph for two data distribution training test ratio of 90:10 and 70:30 on training samples for a bidirectional-LSTM proposed model.

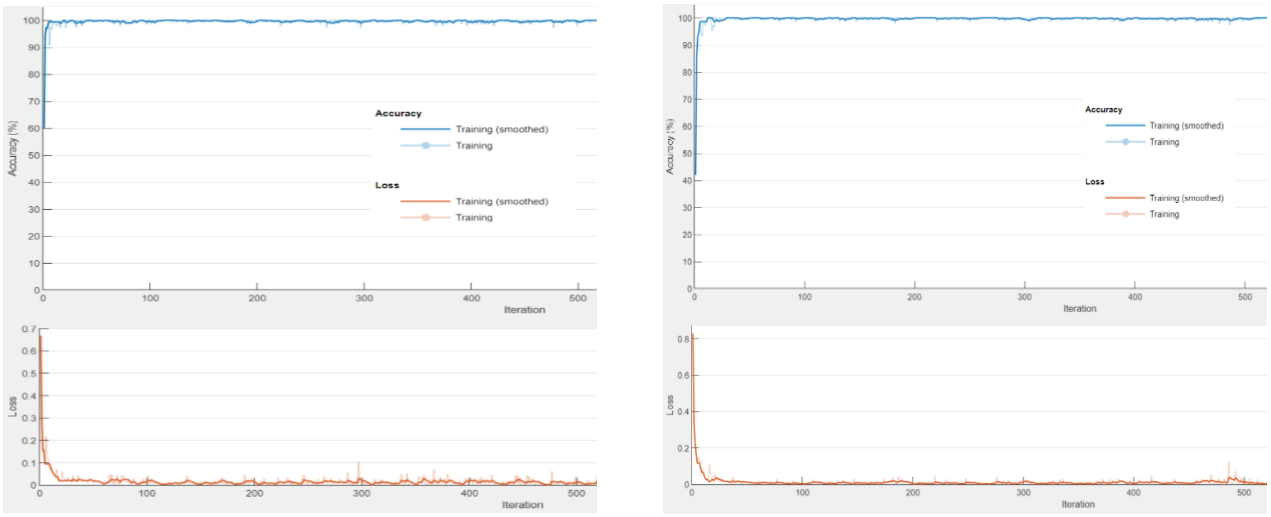

Fig. 5 - Training progress accuracy and loss for (a) 90:10 distribution; (b) 70:30 distribution

Based on both Fig. 5(a) and Fig. 5(b) on 90:10 and 70:30 training test ratio respectively, the top subplot of the training-progress plot represented the training accuracy, which is the classification accuracy on each mini-batch. This value typically increases towards a hundred percent as training progresses successfully. The bottom subplot displays the graph of training loss, which is the cross-entropy loss on each mini-batch. This value generally reduces to zero as training progresses successfully.

The plots will oscillate between values without trending in a certain upward or downward direction if the training is not converged. This oscillation does not improve the training accuracy and does not decrease the training loss. This situation can happen after training starts, or after some preliminary improvement in training accuracy, the plots could plateau. Training options had to be changed to further converge the network. The network has better learned because both MiniBatchSize and InitialLearnRate can be reduced, even though the effects take more time to training. The training accuracy of the classifier is over ninety percent, and it took several hours to train at the end of ten epochs. Overall, it took 123min 35sec of training to complete for 90:10 distributed data. The delivery of training progressed 107min 9 sec at

70:30 distribution. Table 4 show the previous work that using the bidirectional-LSTM on EEG signal for different approaches.

Table 4 - Bidirectional-LSTM on different approaches

Ref	Case Study	Accuracy (%)
[34]	Audio/visual stimuli classification	84.3
[32]	Seizure detection	92.6
[35]	Wind power forecasting	98
This work	Autism Classification	99.6

3.3 Assessment Matrix

Fig. 6(a) and Fig. 6(b) show the confusion matrix on both train and test for 90:10 distribution. While the confusion matrix on both train and test for 70:30 distribution shown in Fig. 7(a) and Fig. 7(b). These figures show Confusion Matrices for Bi-LSTM model and the performance evaluation recorded in Table 5 for both data distribution.

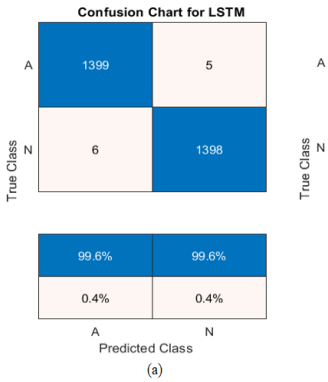

Fig. 6 - 90:10 distribution (a) train; (b) test

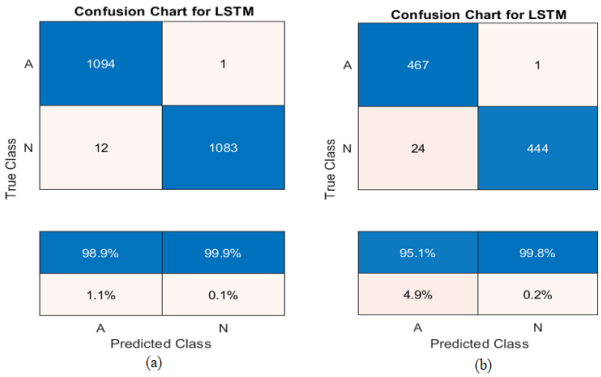

Fig. 7 - 70:30 distribution (a) train; (b) test

Table 5 - Evaluation performance on both data distribution

Performance (100%)	90:10 data distribution		70:30 data distribution	
	Train	Test	Train	Test
Accuracy	99.61	99.68	99.41	97.33
Sensitivity	99.64	99.36	99.91	99.79
Precision	99.15	100	98.92	95.11

Based on Table 5, the used training data updated the bi-LSTM network is classified in three assessment measure. Then, the updated network on testing data is classified and examined the testing accuracy. It is noted that the highest precision obtained for the 90:10 of distributed data on tested data while lowest precision on the other distributed data. Among three performance assessment, the sensitivity had constant percentage of 99 for both data distributions. While, the training accuracy of 99.6% and 99.4%; testing accuracy of 99.7% 97.3% were obtained for 90:10 and 70:30 of data distribution respectively, executed on the EEG database. The exact process repeated on a single LSTM model only for validation scheme of 90:10 distribution. Performance evaluation was recorded in Table 6 for both LSTM and bidirectional-LSTM model and then tabulated in Fig. 8. The bi-LSTM achieved higher accuracy compared to a single LSTM model.

Table 6 - Evaluation performance on LSTM and bi-LSTM for 90:10 validation scheme

Model	Accuracy	Sensitivity	Precision
LSTM			
- Training	93.7	93	93.2
- Validation	93.9	92.8	94.7
Bi-LSTM			
- Training	99.6	99.6	99.2
- Validation	99.7	99.4	100

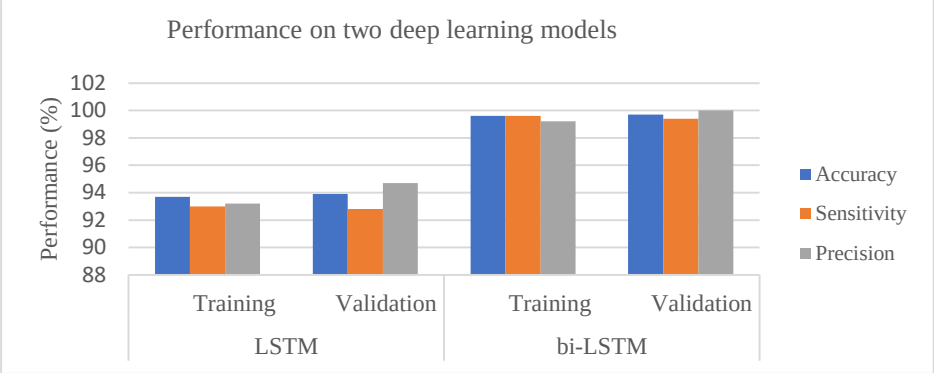

Fig. 8 - The performance assessment on 90:10 validation scheme for both models

4. Conclusions

This research proposed a unique approach autism diagnosis focused on the LSTM-based blocks of deep learning model. The EEG data obtained from the SFARI database were first segmented. This was ideal for nonlinear and non-stationary issues on the brain signal data. A deep learning algorithm network of bi-LSTM developed for both EEG classification, autism and normal (obtained from control individuals), consisting of data training and test distribution information and the result has been mutually decided. Over 97 percent accuracy was achieved for both data distribution, which showed that the approach proposed has an efficient classification capability and performance improvements over a single LSTM method. This study is currently essential and potentially give a significant contribution to neuroscience research. With the best accuracy achieved, this will lead to aid the doctors in diagnosing ASD in children using a quantifiable method rather than depend solely on behavioral observation on the suspected autistic child.

Acknowledgement

Authors acknowledge the support from the Centre for Telecommunication Research and Innovation (CeTRI), Universiti Teknikal Malaysia Melaka (UTeM). This research was supported by UTEM and the Ministry of Higher Education Malaysia (MOHE) through a fundamental research grant (FRGS/2018/FKEKK-CERIA/F00363). Authors are grateful and sincerely appreciate the access given to phenotypic and EEG data on SFARI Base from Simon VIP Foundation.

References

[1] J. Kaur, J. Engkasan, R. Sivanescom, N. Bahar, H. Toran, M. N. Malisa, K. N. Kamarudin. (2015). Technical Report Autism Spectrum Disorder Research in Malaysia, 1-125
[2] E. Jon Baio. (2014). Prevalence of Autism Spectrum Disorder Among Children Aged 8 Years - Autism and Developmental Disabilities Monitoring Network , 11 Sites , United States. MMWR Surveillance Summaries, 63, 1–21
[3] C. A. D. Kevin P. Brady. (2015). Navigating the Current Legal Landscape of the Identification and Eligibility of Children with Autism Spectrum Disorder. Leg. Front. Educ. Complex Law Issues Leaders, Policymakers Policy Implementers, 119–145
[4] M. D. Shen and J. Piven. (2017). Brain and behavior development in autism from birth through infancy. Dialogues Clin. Neurosciences, 19, 325–333
[5] T. Liu, Y. Chen, D. Chen, C. Li, Y. Qiu, and J. Wang. (2017). Altered electroencephalogram complexity in autistic children shown by the multiscale entropy approach. Neuroreport, 28, 169–173
[6] U. R. Acharya, S. L. Oh, Y. Hagiwara, J. H. Tan, and H. Adeli. (2018). Deep convolutional neural network for the automated detection and diagnosis of seizure using EEG signals. Comput. Biol. Med., 100, 270–278
[7] K. Roche. (2019). Electroencephalographic Spectral Power as a Marker of Cortical Function and Disease Severity in Girls With Rett Syndrome. Ann Clin Transl Neurol, 5, 323-332
[8] E. A. Malaia, S. Ahn, and L. L. Rubchinsky (2020). Dysregulation of temporal dynamics of synchronous neural activity in adolescents on autism spectrum. Autism Res., 13, 24–31
[9] J. C. Monterrey, J.Philips, S. Cleveland, S. Tanaka, P. Barnes. (2017). Incidental brain MRI findings in an autism twin study. Autism Res., 10, 113–120
[10] W. J. Bosl, H. Tager-Flusberg, and C. A. Nelson. (2018). EEG Analytics for Early Detection of Autism Spectrum Disorder: A data-driven approach. Sci. Rep., 8, 1–20

[11] W. Jamal, S. Das, K. Maharatna. (2013). Using brain connectivity measure of EEG synchrostates for discriminating typical and Autism Spectrum Disorder. Int. IEEE/EMBS Conf. Neural Eng. NER, 1402–1405
[12] N. A. Ali, A. R. Syafeeza, A. S. Jaafar, M. K. M. Alif. (2020). Autism spectrum disorder classification on electroencephalogram signal using deep learning algorithm. IAES Int. J. Artif. Intell., 9, 91–99
[13] J. Choi, B. Ku, Y. You. (2019). Resting-state prefrontal EEG biomarkers in correlation with MMSE scores in elderly individuals. Sci. Rep., 9, 1–15
[14] E. Grossi, C. Olivieri, and M. Buscema. (2017). Diagnosis of autism through EEG processed by advanced computational algorithms: A pilot study. Comput. Methods Programs Biomed., 142, 73–79
[15] Y. Roy, H. Banville, I. Alburquerque, A. Gramfort. (2018). Deep learning-based electroencephalography analysis: a systematic review. J. Neural Eng., 11–14
[16] Y. M. Y. Han and A. S. Chan. (2017). Disordered cortical connectivity underlies the executive function deficits in children with autism spectrum disorders. Research in Developmental Disability, 61, 19–31
[17] A. Puce and M. S. Hamalainen. (2017). A review of issues related to data acquisition and analysis in EEG/MEG studies. Brain Science, 6, 1-30
[18] J. Neufeld, C. T. Hsu, and B. Chakrabarti. (2019). Atypical reward-driven modulation of mimicry-related neural activity in autism. Front. Psychiatry, 10, 1–8
[19] S. A. Ghani, N. Zaini, H. Norhazman, I. M. Yassin, and M. M. Sani. (2017). Classification of frontal EEG signals of normal subjects to differentiate gender by using Artificial Neural Network. Journal of Telecommunication Electronic Computing. Engineering, 9, 1–3
[20] S. Ibrahim, R. Djemal, and A. Alsuwailem. (2018). Electroencephalography (EEG) signal processing for epilepsy and autism spectrum disorder diagnosis. Biocybern. Biomed. Eng., 38, 16–26
[21] A. Khadem, G. A. Hossein-Zadeh, and A. Khorrami. (2016). Long-Range Reduced Predictive Information Transfers of Autistic Youths in EEG Sensor-Space During Face Processing. Brain Topogr., 29, 283–295
[22] N. F. Harun, N. Hamzah, N. Zaini, M. M. Sani, H. Norhazman, and I. M. Yassin. (2018). EEG classification analysis for diagnosing autism spectrum disorder based on emotions. Journal of Telecommunnication Electronics Computing Engineering, 10, 1–2
[23] K. M. Rispoli, A. L. Malcolm, E. W. Nathanson, and N. E. Mathes. (2019). Feasibility of an emotion regulation intervention for young children with autism spectrum disorder: A brief report. Res. Autism Spectr. Disord., 67, 1-9
[24] V. Bono. (2017). Intensive intervention delivery in autism and early prediction of cognitive outcomes in children using computerized game and wireless EEG in naturalistic setting. Front. Psychiatry, 7, 1-13
[25] R. Al-Jawahiri, E. Milne. (2019). Atypical neural variability in carriers of 16p11.2 copy number variants. Autism Res., 12, 1322–1333.
[26] R. Al-Jawahiri, M. Jones, E. Milne. (2020). Spontaneous neural activity relates to psychiatric traits in 16p11.2 CNV carriers: An analysis of EEG spectral power and multiscale entropy. J. Psychiatr. Res., 1-9
[27] F. Foti, F. Piras, S. Vicari, L. Mandolesi, L. Petrosini, D. Menghini. (2019). Observational learning in low-functioning children with autism spectrum disorders: A behavioral and neuroimaging study. Frontier Psychology, 9, 1–13
[28] A. R. Aslam, M. A. Bin Altaf. (2019). An 8 channel patient specific neuromorphic processor for the early screening of autistic children through emotion detection. Proceeding IEEE International Symposium Circuits Systems, 1-5
[29] B. Glova and I. Mudryk. (2020). Application of Deep Learning in Neuromarketing Studies of the Effects of Unconscious Reactions on Consumer Behavior. IEEE Third Int. Conf. Data Stream Min. Process., 5, 337–340
[30] Y. Zhang, Y. Wang, G. Zhou. (2018.) Multi-kernel extreme learning machine for EEG classification in brain-computer interfaces. Expert Syst. Appl., 96, 302–310
[31] L. Bote-Curiel, S. Muñoz-Romero, A. Gerrero-Curieses, J. L. Rojo-álvarez. (2019). Deep learning and big data in healthcare: A double review for critical beginners. Appl. Sci., 9, 11
[32] X. Hu, S. Yuan, F. Xu, Y. Leng, K. Yuan, Q. Yuan. (2020). Scalp EEG classification using deep Bi-LSTM network for seizure detection. Comput. Biol. Med., 124, 103
[33] J. J. Leblanc, C. A. Nelson. (2016). Deletion and duplication of 16p11.2 are associated with opposing effects on visual evoked potential amplitude. Mol. Autism, 7, 1–7